**Table 2** Number and location of capsular incision in 53 radical prostatectomy specimens with capsular incision according to surgical procedure

Variables	Surgical procedure			P value
	Overall ($n = 53$)	RRP ($n = 21$)	LRP ($n = 32$)	
No of positive capsular incision (%)				0.10
Solitary	11 (20.8)	19 (90.5)	23 (71.9)	
Multiple	42 (79.2)	2 (9.5)	9 (28.1)	
Location of positive surgical margin (%)				
Apex	39 (73.6)	17 (80.9)	22 (68.8)	0.32
Anterior site	11 (20.8)	5 (23.8)	6 (18.8)	0.66
Posterior site	4 (7.5)	0 (0.0)	4 (12.5)	0.092
Bladder neck	12 (22.6)	1 (4.7)	11 (34.4)	0.012

RRP Open radical prostatectomy, *LRP* Laparoscopic radical prostatectomy
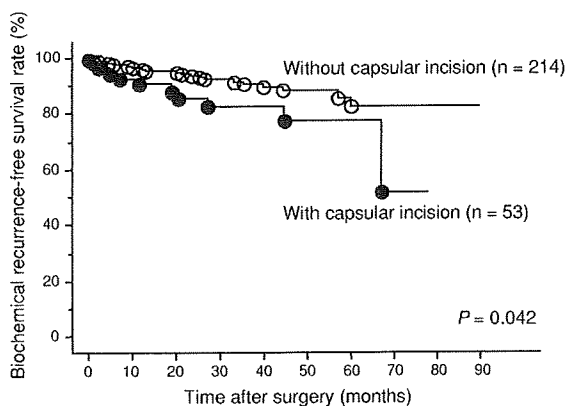
Fig. 1 Comparison of biochemical recurrence-free survival between patients with and without capsular incision who underwent radical prostatectomy for clinically organ-confined prostate cancer

of an individual surgeon [2–4]. Positive surgical margin could also occur even if tumor tissue is localized within the prostate by iatrogenic capsular incision at RP [5]; however, it remains controversial whether capsular incision influences the prognosis of patients with prostate cancer treated with RP [5–10]. For example, Barocas et al. [5] did not show significant difference in the likelihood of early recurrence between isolated capsular incision and other specimen-confined disease, while Shuford et al. [10] reported that the presence of capsular incision has a prognostic impact similar to pT3a disease with positive surgical margin. In the present study, therefore, we retrospectively reviewed clinicopathological data from Japanese men who underwent RP and were pathologically diagnosed as having organ-confined

disease focusing on the significance of capsular incision.

We initially would like to emphasize various definitions of capsular incision used in previous studies. As in the present study, some studies defined capsular incision as margin positive and pathologically organ-confined disease, where the surgeon inadvertently developed the resection plane within rather than exterior to the prostate; hence, these studies regarded not only exposed tumor tissues but also adjacent benign glands as capsular incision [6, 8, 9, 11]. Others broadened the definition to that including other equivocal margins [10, 12]. In addition, it would be a challenging problem to distinguish capsular incision from positive margin with extraprostatic extension at the apex where the histological boundaries of the prostate are vague; accordingly, some series excluded or restricted positive apical margin from capsular incision [5, 10]. Collectively, these findings suggest the difficulty in uniformly interpreting the previously reported data concerning capsular incision.

As shown in Table 4, the incidences of capsular incision noted in pT2 disease varies widely ranging from approximately 2 to 40% in the literature [6–10]. In this series, capsular incision was detected in 19.9% of patients with pathologically confirmed pT2 prostate cancer, which is relatively high compared with those in previous series. This outcome could be mainly explained by the simultaneous analysis of both RRP and LRP specimens; that is, as previously described [20], our surgical skill in LRP may be immature compared with that in RRP, resulting in a

Table 3 Univariate and multivariate analyses of several parameters as predictors of biochemical recurrence

Variables	Univariate analysis		Multivariate analysis	
	Hazard ratio	P value	Hazard ratio	P value
Age (years) (less than 70 vs 70 or greater)	0.77	0.47	–	–
PSA (ng/ml) (less than 10 vs 10 or greater)	3.38	0.0010	2.70	0.012
Surgical procedure (RRP vs LRP)	0.81	0.92	–	–
Pathological stage (pT2a or pT2b vs pT2c)	1.22	0.67	–	–
Gleason score (7 or less vs 8 or greater)	5.01	0.0087	2.66	0.12
Lymphatic invasion (negative vs positive)	1.64	0.19	–	–
Microvenous invasion (negative vs positive)	2.09	0.11	–	–
Perineural invasion (negative vs positive)	2.45	0.039	1.93	0.14
Capsular incision (negative vs positive)	2.11	0.044	1.71	0.17

PSA Prostate-specific antigen, *RRP* Open radical prostatectomy, *LRP* Laparoscopic radical prostatectomy

Table 4 Comparison of studies focusing on capsular incision

	No. of patients	No. of patients with capsular incision (%)	Definition of biochemical recurrence (ng/ml)	Biochemical recurrence-free probability		
				Without capsular incision (%)	With capsular incision (%)	Interval after surgery (year)
Ohori et al. [6]	247	23 (9.3)	>0.4	95	100	5
Boccon-Gibot et al. [7]	51	19 (37.3)	>0.1	100	63	3
Cheng et al. [8]	298	72 (24.1)	>0.2	90	78	5
Shuford et al. [10]	147	18 (12.2)	>0.2	96	65	3
Chaung et al. [9]	7,666	135 (1.8)	>0.2	97	71	5
Current study	267	53 (19.9)	>0.2	91	83	3

significantly higher incidence of capsular incision in the LRP group than that in the RRP group (i.e., 26.2 vs 14.5%). Furthermore, the anatomical location where capsular incision is most likely to occur also varies among previous studies [9, 10, 12]. For example, Chuang et al. [9] reported that capsular incision into the prostate most frequently occurred in the neurovascular bundle regions; however, in the present study, the apex was the most common site of capsular incision irrespective of surgical procedure for RP. These controversial outcomes may, at least in part, reflect differences in the definition of capsular incision at the apex, the histological assessment of RP specimens at the apical region and the proportion of preservation of neurovascular bundles during RP.

It is of interest to investigate the prognostic significance of capsular incision at RP. In this series, recurrence-free survival in patients with capsular incision was significantly poorer than that in those without capsular incision, and despite the lack of

independent significance, capsular incision was identified as one of the significant factors predicting time to biochemical recurrence. However, the previous data associated with the prognostic impact of capsular incision are conflicting [6–10] (Table 4). For example, Shuford et al. [10] reported that patients with capsular incision were greater than 8- and 6-times more likely to have biochemical recurrence than those with pT2 and pT3a disease without capsular incision, respectively, whereas there was no adverse prognostic effect of capsular incision in the studies by Ohori et al. [6]. Similar to outcomes regarding the incidence of capsular incision, a number of factors could be involved in the difference in prognostic significance of capsular incision among previously reported outcomes, including patient selection, surgical technique, the method of pathological examinations, and the definition of biochemical recurrence. Collectively, these findings suggest that, although it would be requited to make an

effort to clarify the prognostic impact of capsular incision at RP, urologists should further refine the surgical technique for RP to avoid iatrogenic incision into the prostate irrespective of the significance of RP considering the possible relation between capsular incision and an unfavorable biochemical outcome.

In conclusion, the current findings showed that capsular incision, which was detected in approximately 20% of RP specimens from men with pathologically organ-confined prostate cancer, appeared to have an adverse impact on biochemical outcome following RP. However, previously reported outcomes concerning the prognostic significance of capsular incision remain controversial; therefore, it would be absolutely necessary to perform a prospective study under uniform conditions to draw conclusive findings on the significance of capsular incision at RP.

References

1. Hull GW, Rabbani F, Abbas F et al (2002) Cancer control with radical prostatectomy alone in 1, 000 consecutive patients. J Urol 167:528–534. doi:10.1016/S0022-5347(01)69079-7
2. Graefen M (2006) The positive surgical margin after radical prostatectomy—why do we still not really know what it means? Eur Urol 50:199–201. doi:10.1016/j.eururo.2006.02.016
3. Khan MA, Partin AW (2005) Surgical margin status after radical retropubic prostatectomy. BJU Int 95:281–284. doi:10.1111/j.1464-410X.2005.05282.x
4. Chang SS, Cookson MS (2006) Impact of positive surgical margins after radical prostatectomy. Urology 68:249–252. doi:10.1016/j.urology.2006.03.053
5. Barocas DA, Han M, Epstein JI et al (2001) Does capsular incision at radical retropubic prostatectomy affect disease-free survival in otherwise organ-confined prostate cancer? Urology 58:746–751. doi:10.1016/S0090-4295(01)01336-X
6. Ohori M, Wheeler TM, Kattan MW et al (1995) Prognostic significance of positive surgical margins in radical prostatectomy specimens. J Urol 154:1818–1824. doi:10.1016/S0022-5347(01)66792-2
7. Boccon-Gibod L, Ravery V, Vordos D et al (1998) Radical prostatectomy for prostate cancer: the perineal approach increases the risk of surgically induced positive margins and capsular incisions. J Urol 160:1383–1385. doi:10.1016/S0022-5347(01)62543-6
8. Cheng L, Darson MF, Bergstralh EJ et al (1999) Correlation of margin status and extraprostatic extension with progression of prostate carcinoma. Cancer 86:1775–1782. doi:10.1002/(SICI)1097-0142(19991101)86:9<1775::AID-CNCR20>3.0.CO;2-L
9. Chuang AY, Nielsen ME, Hernandez DJ et al (2007) The significance of positive surgical margin in areas of capsular incision in otherwise organ confined disease at radical prostatectomy. J Urol 178:1306–1310. doi:10.1016/j.juro.2007.05.159
10. Shuford MD, Cookson MS, Chang SS et al (2004) Adverse prognostic significance of capsular incision with radical retropubic prostatectomy. J Urol 172:119–123. doi:10.1097/01.ju.0000132137.02846.ec
11. Epstein JI (1996) Incidence and significance of positive margins in radical prostatectomy specimens. Urol Clin North Am 23:651–663. doi:10.1016/S0094-0143(05)70343-8
12. Watson RB, Civantos F, Soloway MS (1996) Positive surgical margins with radical prostatectomy: detailed pathological analysis and prognosis. Urology 48:80–90. doi:10.1016/S0090-4295(96)00092-1
13. Huland H, Hammerer P, Henke RP et al (1996) Preoperative prediction of tumor heterogeneity and recurrence after radical prostatectomy for localized prostatic carcinoma with digital rectal, examination prostate specific antigen and the results of 6 systematic biopsies. J Urol 155:1344–1347. doi:10.1016/S0022-5347(01)66262-1
14. Walsh PC (1994) Radical prostatectomy: a procedure in evolution. Semin Oncol 21:662–671
15. Koch MO (2000) Management of the dorsal vein complex during radical retropubic prostatectomy. Semin Urol Oncol 18:33–37
16. Guillonneau B, Vallancien G (2000) Laparoscopic radical prostatectomy: the Montsouris technique. J Urol 163:1643–1649. doi:10.1016/S0022-5347(05)67512-X
17. Hara I, Kawabata G, Miyake H et al (2002) Feasibility and usefulness of laparoscopic radical prostatectomy: Kobe University experience. Int J Urol 9:635–640. doi:10.1046/j.1442-2042.2002.00530.x
18. LinksHu JC, Gold KF, Pashos CL et al (2003) Role of surgeon volume in radical prostatectomy outcomes. J Clin Oncol 21:401–405. doi:10.1200/JCO.2003.05.169
19. Eastham JA, Kattan MW, Riedel E et al (2003) Variations among individual surgeons in the rate of positive surgical margins in radical prostatectomy specimens. J Urol 170:2292–2295. doi:10.1097/01.ju.0000091100.83725.51
20. Terakawa T, Miyake H, Tanaka K et al (2008) Surgical margin status open versus laparoscopic radical prostatectomy specimens. Int J Urol (in press)

Biomarkers, Genomics, Proteomics, and Gene Regulation

Staphylococcal Nuclease Domain-Containing Protein 1 as a Potential Tissue Marker for Prostate Cancer

Hidetoshi Kuruma,* Yuko Kamata,†
Hiroyuki Takahashi,‡ Koji Igarashi,§
Takahiro Kimura,* Kenta Miki,* Jun Miki,*
Hiroshi Sasaki,* Norihiro Hayashi,*
and Shin Egawa*

From the Departments of Urology, Oncology,† Institute of DNA
Medicine, and Pathology,‡ Jikei University School of Medicine,
Tokyo, Japan; and the Bioscience Division,§ Reagent Development
Department, AIA Research Group, Tosoh Corporation,
Kanagawa, Japan*

**Using high molecular-weight proteomic analysis, we previously showed that Staphylococcal nuclease domain-containing protein 1 (SND1) is highly expressed in recurrent androgen-insensitive prostate cancer tissues. SND1 is a component of the RNA-induced splicing complex that mediates RNA interference, leading to degradation of specific mRNAs. The objective of this study was to further characterize SND1 expression and to investigate its biological potential in prostate cancer. Radical prostatectomy specimens were obtained from 62 prostate cancer patients. SND1 immunohistochemical staining patterns were evaluated using an in-house polyclonal antibody. We confirmed SND1 mRNA expression in prostate cancer cells using an *in situ* hybridization technique. To determine the importance of SND1 mRNA, we knocked down SND1 *in vitro* with small interfering RNA and observed a significant decrease in cell growth. SND1 was expressed in 60 of 62 prostate cancers (97%), appearing in the cytoplasm as small, granular structures; it was also present at high levels in prostate cancer specimens, while in hyperplasia specimens and normal epithelium, it was weakly or negatively expressed. SND1 expression intensity increased with increasing grade and aggressiveness of the cancer. As SND1 mRNA was overexpressed in cancer cells, the growth of these cells was suppressed following SND1 knockdown *in vitro*, thus representing a promising prostate cancer biomarker and therapeutic target. *(Am J Pathol 2009, 174:2044–2050; DOI: 10.2353/ajpath.2009.080776)*

Prostate cancer is extremely common in Western countries affecting, one in every six men in their lifetime. Most prostate cancers initially require androgen for growth, and thus androgen-depletion therapy leads to marked tumor regression by apoptosis. This therapy is unfortunately only palliative, and some cancer cells develop the ability to proliferate even in the absence of circulating serum androgen. These cells culminate in what is considered an androgen-independent phenotype. We have previously investigated alterations in expression of several proteins in recurrent androgen-dependent prostate cancer LNCaP cells after androgen suppression by proteomic analysis.[1] Staphylococcal nuclease domain-containing protein 1 (SND1), also named Epstein-Barr virus-encoded transcription factor 2 co-activator p100, or Tudor staphylococcal nuclease, was found to exhibit a visually distinct pattern of up-regulation (1.5-fold by densitometric measurement) in androgen-independent cancers, as compared with androgen-dependent cancers in our previous study. This observation prompted us to further investigate the clinical relevance of this particular protein.

SND1 was originally reported in 1995 as a component of the RNA-induced splicing complex that mediates RNA interference in *C. elegans*, leading to degradation of specific mRNA.[2] In mammalian cells, RNA interference occurs subsequent to loading microRNAs (miRs) into RNA-induced splicing complex where they guide mRNA degradation or translation silencing depending on the complementarity of the target.[3] Activation of RNA interference pathway based on miR machinery is very important in oncogenesis and cancer development. Volinia et al[4] reported that miR array of several solid cancers revealed an almost global up-regulation of miRs as a common feature of oncogenesis in many tissue types. Specifically in prostate adenocarcinoma, 39 of 45 differ-

2044

ent expressed miRs are up-regulated. An RNase III endonuclease, named dicer, is an essential component of the miR machinery, and its over-expression means activation of RNA interference to degrade target mRNAs. Chiosea et al[5] reported that dicer is up-regulated in prostate cancer. They discussed that dicer may play a role in the early steps of prostate cancer development, probably by potentiating an almost miR up-regulation.

Along with dicer, SND1 is also the central component of the miR machinery. Our previous report revealed SND1 was up-regulated in androgen independent phenotype of prostate cancer. As the one of main player of miR machinery, SND1 may engage early carcinogenesis, and further androgen independency. If it is true, SND1 is likely a marker for prostate cancer and may be used in the detection of the aggressive phenotype. To verify this hypothesis, we validated SND1 expression in surgical specimens and compared its expression pattern and association with histological and clinical parameters in prostate cancer to that α-methylacyl-coenzyme A racemase (AMACR). AMACR is a clinically applicant tissue marker protein, which shows high sensitivity for prostate cancer and is useful for a pathologically doubtful case.[6]

Materials and Methods

Patients and Tissue Samples

From 1993 to 2003, 174 patients with prostate cancer received radical retropubic prostatectomy at the Jikei University Hospital. Ninety-three patents received neoadjuvant hormone therapy. Unfortunately, due to the preservation state of some specimens, 21 patients were excluded from this study. Study approval was granted by the Jikei University Ethics Committee Institutional Review Broad.

Table 1 lists characteristics of the patients. Preoperative prostate specific antigen (PSA) was quantified by Tosoh PSA assay (Tosoh Corporation, Tokyo, Japan). Biochemical failure was defined as two consecutive PSA increases ≥0.2 ng/ml. The date of failure was considered to be the time of the first increase.

Morphological Evaluation

All resected specimens were fixed in 10% neutral buffered formalin and embedded in paraffin. Tumors were graded by a single pathologist (H.T.) using the original Gleason grading system.[7] Pathological stage was determined by the same pathologist according to the 2002 TNM classification system.[8] If high-grade prostatic intraepithelial neoplasia (HGPIN) or hyperplasia presented in the same specimen, the corresponding areas were also marked.

Preparation of Polyclonal Antibody to SND1

The antigen peptide RPASPATETVPAFSERTC corresponds to an internal sequence of SND1 (amino acids 423 to 440, Swiss-Prot; *http://br.expasy.org/uniprot/Q7KZF4*). The anti-

Table 1. Patient Demographics

No. pts.	62
Mean age (range)	65.1 (51–76)
Mean PSA (ng/ml, range)	13.4 (3.69–41.6)
No. PSA (ng/ml) (%)	
<10.0	21 (33.9)
10.0–20.0	29 (46.8)
>20.0	12 (19.4)
No. Gleason score (%)	
2–6	17 (27.4)
7	30 (48.4)
8–10	15 (24.2)
No. highest Gleason pattern (%)	
1	0 (0)
2	7 (11.3)
3	33 (53.2)
4	15 (24.2)
5	7 (11.3)
No. pathological stage (%)	
pT2a	6 (9.7)
pT2b	32 (51.6)
pT3a	19 (30.6)
pT3b	5 (8.1)
No. pos. capsular invasion (%)	21 (33.9)
No. pos. surgical margin (%)	31 (50.0)

No. pts, number of patients, PSA, prostate specific antigen, pos., positive.

gen peptide was conjugated to the carrier protein keyhole limpet hemocyanin and used to immunize *Japanese White* rabbits. The immune response was monitored by enzyme-linked immunosorbent assay and immunoglobulins from high-titer sera were collected with a protein G-immobilized column. The antibody was purified and isolated by affinity purification with a column using immobilized antigen peptide. This antibody was used in the following experiments.

Immunohistochemical Staining

Immunohistochemical (IHC) analysis was performed for the index or largest cancer focus in each surgical specimen. Immunoreactivity of SND1 was compared with that of another commercially available marker, AMACR, for which the rabbit monoclonal antibody P504S (Dako Japan, Tokyo, Japan) was used. Formalin-fixed, paraffin-embedded tissue sections were deparaffinized and rehydrated through a xylene and ethanol series and then treated with 3% hydrogen peroxide for 5 minutes to block endogenous peroxidase activity. Subsequently, slides were washed in distilled water, and then pretreated with citrate buffer solution (pH 6.0) in a microwave at 800 watts power for 10 minutes. After cooling, slides were washed and labeled. Since there was not internal control for adjusting IHC staining, we stained all specimens at the same moment using an automatic staining system; the Ventana Nexus automated stainer with Ventana reagent (Ventana Medical Systems, Inc., Tucson, AZ). The anti-SND1 antibody and P504S were applied at 0.6 mg/ml and a dilution of 1:100, respectively, for 32 minutes at 37°C, and the following detection and visualization procedures were performed according to the manufacture's protocol using the Ventana 3,3-diaminobenzidine
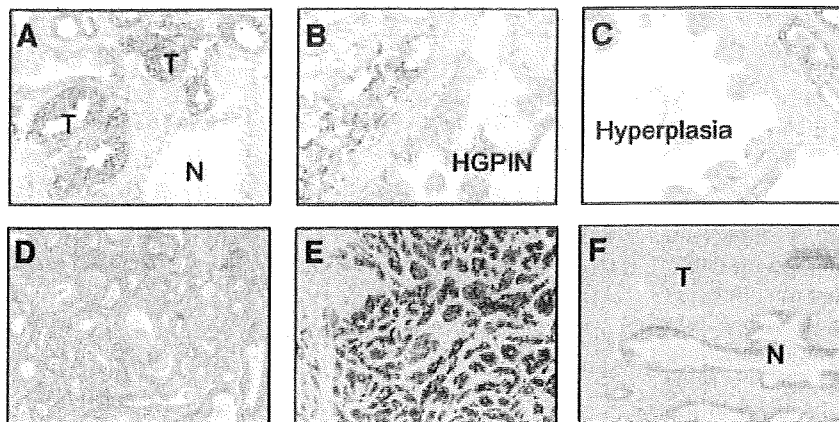
Figure 1. SND1 expression in cancerous prostate tissue. SND1 was localized in the cytoplasm of cancer cells, but not expressed in normal gland (A). In HGPIN (B) and hyperplasia (C), SND1 expression was negative or weakly positive. Cancer of Gleason pattern 2 was stained weakly (D), whereas Gleason pattern 5 was stained strongly (E). Negative control was not stained both cancer and normal gland (F). T: cancer, N: normal gland.

Basic Detection kit (Ventana Medical Systems, Inc.), which includes a universal biotinylated IgG secondary antibody (anti-mouse and anti-rabbit antibodies), avidin horseradish peroxidase, and 3,3-diaminobenzidine. After staining, slides were counterstained with hematoxylin. The specificity of the binding was confirmed by negative staining using rabbit nonimmune serum as a primary antibody.

An IHC score of 1 was assigned for variable or weak cytoplasmic staining, a score of 2 for moderate, apical granular cytoplasmic staining, and a score of 3 for strong cytoplasmic staining. No staining (negative IHC) received a score of 0. The patient's score was the highest score in the index tumor, which was assigned by a single pathologist (H.T.) without access to clinical information. The IHC score was also blindly marked by another independent researcher (H.K.), and then each result was merged. In the case of different score, the two individuals discussed and concluded on a fixed IHC score. Normal area was chosen from an area far from the cancerous area. If the specimen contained HGPIN or hyperplasia lesions, these were evaluated by the same manner.

In Situ *Hybridization*

In situ hybridization of SND1 was conducted as previously described.[9] Complementary DNA was prepared using 1 μg of total RNA isolated from the cell lysate using Isogen (Nippon Gene Co. Ltd, Tokyo, Japan). Primers used to amplify specific gene products were: SND1 forward, 5'-TCATCAAGATGGTCCTCTCA-3'; and SND1 reverse, 5'-CTTAATACGACTCACTATAGGGTGCAATGTT-TTCCCCATTGG-3'. The PCR products were obtained using the One-Step reverse transcription (RT)-PCR kit (QIAGEN Japan, Tokyo, Japan) in accordance with the manufacturer's protocol. The PCR product of SND1 was transcribed using a digoxigenin RNA labeling kit (Roche Diagnostics, Basel, Switzerland) to produce a complementary RNA probe. After removing paraffin from paraffin-embedded sections with a xylene and ethanol series, the complementary RNA probe was reacted overnight at 50°C. After a standard blocking treatment, anti-rabbit digoxigenin/horseradish peroxidase antibody (Dako Japan, Kyoto, Japan) was reacted for 15 minutes. The

antibody-bound SND1 mRNA was then visualized using the GenPoint System (Dako Japan) in accordance with the manufacturer's protocol.

Cell Lines

The human prostate cancer cell line PC-3 was obtained from the American Type Culture Collection (Rockville, MD). Cells were cultured as a monolayer in Roswell Park Memorial Institute 1640 medium (Invitrogen Japan, Tokyo, Japan) supplemented with 10% fetal bovine serum. Cultures were maintained at 37°C in an atmosphere of humidified air with 5% CO_2.

Small Interfering RNA-Expressing Constructs and Knockdown of SND1

We used small interfering RNAs (siRNAs) predesigned by B-Bridge International (Mountain View, CA) to knock down SND1 mRNA. The target sequences for SND1 are 5'-GGGAGAACACCCAGGATAA-3' (Si-1) and 5'-CAG-
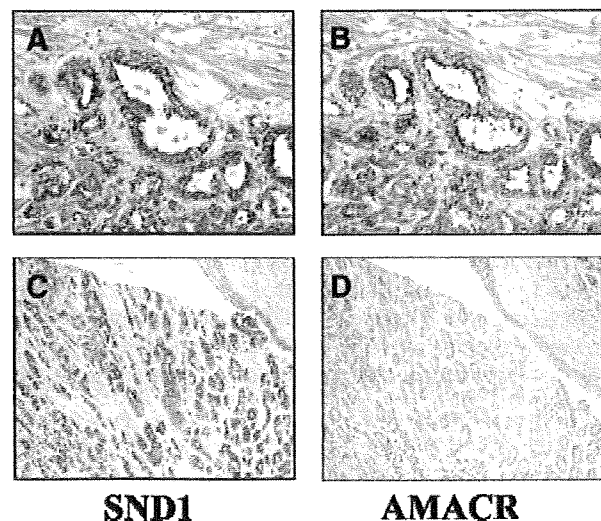
SND1   **AMACR**

Figure 2. The expressions of SND1 and AMACR in prostate cancer. The expression of AMACR was similar to SND1 (A, B), but in some cases, SND1 positive cancer cells (C) did not show AMACR expression (D).

Table 2.   Comparison of IHC Scores between SND1 and AMACR Stratified by Final Diagnosis, PSA, Gleason score, and Pathological Stage for 62 Radical Prostatectomy Specimens

IHC score	SND1						AMACR					
	0	1	2	3	Mean	P^*	0	1	2	3	Mean	P^*
No. cancer total	2	14	40	6	1.8	<0.0001	0	6	25	31	2.4	<0.0001
No. PSA (ng/ml)						0.012						0.85
<10	0	9	10	1	1.6		0	2	9	9	2.4	
10<20	2	5	20	1	1.7		0	2	9	9	2.4	
>20	0	0	9	3	2.3		0	0	6	6	2.5	
No. Gleason score						0.025						0.65
2<6	1	7	9	0	1.5		0	2	8	7	2.3	
7	1	4	23	2	1.9		0	4	10	16	2.4	
8<10	0	3	8	4	2.1		0	0	7	8	2.5	
No. pathological stage						0.95						0.60
pT2	1	8	25	4	1.8		0	4	16	18	2.4	
pT3	1	5	16	2	1.8		0	2	9	13	2.5	
No. HGPIN	7	31	4	0	0.93		4	33	5	0	1.0	
No. hyperplasia	37	14	0	0	0.24		27	24	0	0	0.47	
No. normal gland	47	15	0	0	0.27		34	28	0	0	0.45	

$^*P$ value for differences mean score among groups of cancer, HGPIN, hyperplasia and normal gland, and each group of PSA. Gleason scores were assessed using the Kruskal-Wallis test. P value for difference between pT2 and pT3 was assessed using the Mann-Whitney U test.

CAAAGGTCTAGCCACA-3′ (Si-2). PC-3 cells were cultured in a 6-well culture plate at 5 × 10^5 cells/well. On the following day, the cells were transfected with 0.1 mmol/well of siRNAs using DharmaFECT 2 transfection kit (Dharmacon, Lafayette, CO). As a negative control, cells were treated with an irrelevant siRNA, (5′-ATCCGCGC-GATAGTACGTATT-3′, B-Bridge international). Viable cells were counted 72 hours after transfection. The effect of SDN1 knockdown was expressed as percentage of negative control.

Real-Time Quantitative RT-PCR

Interference with SND1 mRNA expression was confirmed by real-time quantitative RT-PCR, which was performed with TaqMan Gene Expression Assay (Applied BioSystems, Werrington, UK). Total RNA was extracted using the Ambion *mir*Vana PARIS kit (Applied BioSystems). Five-hundred ng of total RNA was used for first-strand cDNA synthesis by SuperScript VILO (Invitrogen, Tokyo,

Japan). The cDNA (5 ng of the total RNA) and TaqMan real-time primers and probes were used for amplification. A set of primers and a probe for each gene tested was obtained from Applied Biosystems (SND1 assay ID: Hs00205182-m1, β-actin: TaqMan PreDeveloped Assay Reagents). Fluorescence was detected using the ABI PRISM 7300 sequence detection system (Applied Biosystems). The relative mRNA expression level of each gene for each patient was normalized for input RNA against β-actin expression in the sample.

Statistical Analysis

Clinicopathological parameters were divided into groups; age (<70 or ≥70-year-old), PSA (<10, 10 to 20, or >20 ng/ml), Gleason score (2 to 6, 7, or 8 to 10), and pathological stage (pT2 or pT3). The correlation between SND1 or AMACR expression levels and clinicopathological variables was evaluated using the Mann-Whitney U test for comparing between two groups and Kruskal-Wallis test for three or more groups. The probability of biochemical failure was determined using the Kaplan-Meier method. Differences in survival curves were compared using the log-rank test. The Cox proportional hazards regression model was used for multivariate analysis of biochemical
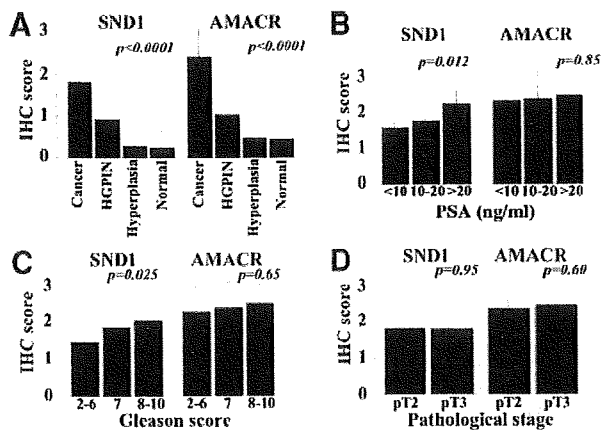
Figure 3. Relative expression of SND1 and AMACR by IHC score stratified by (**A**) histological findings including cancer, HGPIN, hyperplasia and normal glands, (**B**), serum PSA levels, (**C**) Gleason score, and (**D**). pathological stage. Column, mean; bars, SD.
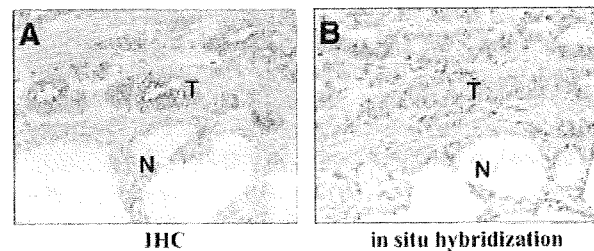
Figure 4. *In situ* hybridization of a surgical specimen for prostate cancer. **A:** IHC shows SND1 was highly expressed in cancer cells (T) but almost negative in noncancerous cell (N). **B:** *In situ* hybridization shows SND1 mRNA was highly expressed in cancer cells (T) but was almost negative or weakly positive in normal luminal cells (N). IHC, immunohistochemistry.

failure risk. Student's *t*-test was used for comparisons of differences between knocked-down cells and negative controls. A difference was considered statistically significant at $P < 0.05$. All analyses were performed with StatView 5.0 statistical package (SAS Institute Inc., Cary, NC) except for Student's *t*-test, which was performed with Excel 2007 software (Microsoft Corporation, Richmond, WA).

Results

IHC Analysis of SND1 and AMACR

IHC staining revealed SND1 predominantly in the cytoplasm of cancer cells, typically as small granular structures (Figure 1A–F). The expression of AMACR was similar, but some SND1-positive cancer cells did not show AMACR expression (Figure 2A–D). In prostate cancer specimen, SND1 and AMACR expression were detected in 60 (97%) and 62 (100%) of a total 62 cases, respectively. However, both SND1 and AMACR were either weakly or not at all expressed (IHC score 0 to 1) in all benign prostatic glands, including the hyperplastic glands and normal luminal cells. In HGPIN, SND1, and AMACR were detected in 83.3% (35/42) and 90.5% (38/42) of the specimens, respectively, though expression was weak in most cases. Overall, order ranked staining from strong to weak appeared as cancer, HGPIN, and benign (Figure 1). The IHC scores in cancer, HGPIN, hyperplasia, and normal luminal cells were 1.7, 0.93, 0.24, and 0.27, ($P < 0.0001$ by Kruskal-Wallis tests) for SND1, respectively, and 1.9, 1.0, 0.47, and 0.45, ($P < 0.0001$ by Kruskal-Wallis tests) for AMACR, respectively (Table 2).

The intensity of SND1 immunoreactivity showed distinct correlation with Gleason score; more intense immunoreactivity being associated with higher specimen score ($p = 0.025$; Figure 3A and C, and Table 2). Expression of SND1 was also associated with high PSA but not with pathological T stage (Figure 3, A, B, and D). By contrast, AMACR showed no relationship with any clinicopathological parameters including Gleason score, PSA level, and pathological T stage.

SND1 mRNA Expression in Tissues

Ten slides were selected randomly for confirmation of SND1 mRNA expression in surgical specimens by *in situ* hybridization. In all selected slides SND1 protein was found positive in cancer cells and negative to weak in expression in normal luminal cells. The intensity of mRNA signals was very similar to the IHC findings. That is, SND1 mRNA was highly expressed in the cytoplasm of cancer cells but was negative to weak in noncancerous cells (Figure 4, A–B).

Knockdown of SND1 by siRNA

Endogenous expression of SND1 mRNA was knocked down by two types of specifically designed siRNAs (Si-1 and Si-2) in the prostate cancer PC-3 cell line. Real-time quantitative RT-PCR showed Si-1 and Si-2 significantly
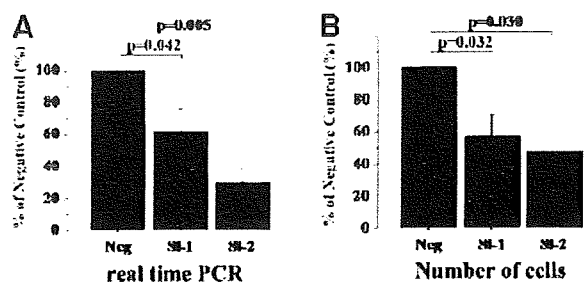
Figure 5. Effect of knockdown of SND1 mRNA in PC-3 cells. A: Real-time quantitative RT-PCR showed SND1-specified siRNAs (Si-1, Si-2) significantly decreased SND1 gene expression. B: Cell growth of prostate cancer was suppressed comparing to negative control by knockdown with siRNAs. Column, mean; scale bars = SD.

decreased gene expression of SND1, by 62.1% and 30.0%, respectively, compared with the negative control ($p = 0.042$ and 0.005, respectively). In PC-3 cells where SND1 had been knocked down by Si-1 or Si-2 growth was significantly suppressed (by 56.7% and 47.3%, respectively) as compared with control cells, (Figure 5A-B; $p = 0.032$ and 0.030, respectively).

Results of Multivariate Analysis for Biochemical Failure after Surgery

Of 62 patients, 14 were lost during follow-up due to patient noncompliance. No deaths occurred throughout the study. At a median follow-up time from prostatectomy to biochemical failure of 35 months (range, 3 to 113 months) biochemical failure had occurred for 49.1% of these patients. In univariate Kaplan-Meier analysis, primary Gleason grade was associated significantly with biochemical failure ($p = 0.047$). In an exploratory multi-

Table 3. Univariate and Multivariate Analysis (Cox Regression Model) for Biochemical Failure

Variable	HR (95% CI)	P
Univariate analysis		
pT stage (≥pT3 vs. <pT3)	1.004 (0.463, 2.175)	0.99
Primary Gleason grade (≥4 vs. <4)	2.184 (1.011, 4.721)	0.047*
Gleason score (≥7 vs. <7)	2.493 (0.926, 6.712)	0.071
Capsular invasion (positive versus negative)	1.425 (0.654, 3.107)	0.37
SND1 IHC score (≥2 vs. <2)	1.627 (0.612, 4.325)	0.33
AMACR IHC score (≥3 vs. 3)	0.761 (0.348, 1.660)	0.49
Multivariate analysis		
pT stage (≥pT3 vs. <pT3)	0.283 (0.089, 0.904)	0.033*
Capsular invasion (positive versus negative)	3.324 (1.031,10.139)	0.044*
SND1 IHC score (≥2 vs. <2)	2.228 (0.643, 7.717)	0.21
AMACR IHC score (≥3 vs. 3)	0.391 (0.144, 1.059)	0.065

*$P < 0.05$.

variate analysis that included age, PSA, pathological stage, capsular invasion, surgical margin, primary Gleason grade, SND1 intensity, and AMACR intensity, pathological stage and capsular invasion SND1 had independent prognostic significance. However, high SND1 expression was not an independent predictor for biochemical failure after radical prostatectomy ($p = 0.21$, Table 3).

Discussion

We have shown evidence for the diagnostic potential of SND1 in prostate surgical specimens equivalent or better than that of AMACR. There have been numerous reports indicating the effectiveness of AMACR for identifying cancer, which have resulted to its use in the clinical setting.[10] However, since AMACR staining is unstable and the test shows unsatisfactory specificity, it is considered insufficient for use as an independent tumor diagnostic marker. In cases with difficult pathological diagnosis, an antibody cocktail containing AMACR together with the basal cell markers 34βE12 and p63 is available for cancer confirmation.[11] SND1 offers a promising new tissue marker, however its specificity, although better than that of AMACR, is still not sufficient for use as a sole marker. SND1 and AMACR do show different expression in some cases (Figure 2, C–D) and therefore the possibility of SND1 joining the cocktail of pathologically useful tissue markers that includes AMACR, 34βE12, and p63 is favored.

At this time, the Gleason score of biopsy specimens is the most powerful predictor of prostate cancer progression, and is an essential parameter in nomograms for predicting clinically insignificant cancer.[12] However, since the Gleason grading system is based solely on glandular architecture, small specimens such as needle biopsy samples often show poor interpathologist reproducibility.[13] Moreover, scores are based on the pathologist's subjective impression and experience. Even in surgical specimens, the scores assigned by trained observers disagree with those previously assigned in over 70% of cases.[14] Hence, a new tissue marker that reflects grade of malignancy would contribute significantly to the objective assessment of prostate cancer. We found that prostate cancer cells with higher Gleason score exhibited more intense SND1 expression than did those with lower grades (Figure 3, A and C). It seems reasonable to suppose that SND1 is related with aggressiveness of prostate cancer. To put in clinical language, although some of Gleason 8 to 10 cancers only showed weak expression, SND1 may offer an important role in distinguishing the presence of a more aggressive and clinically significant phenotype. In our study, statistical significance was not observed through multivariate analysis to identify high SND1 expression as an independent predictor of biochemical failure after radical prostatectomy, and this may be attributed to the small sample size used. Since statistical significance was also not found for specimen Gleason score in this study, the small sample size may have contributed to this overall observation of SND1 not being an independent predictor of biochemical

failure. Follow-up studies with a larger sample population are necessary to investigate this.

siRNAs specifically knocked down SND1 mRNA and effectively inhibited cell proliferation of PC-3 prostate cancer cells (Figure 5). Reports of this molecule's function in other settings have recently appeared and may provide insight as to its function in prostate cancer cells. SND1 was previously identified as an enhancer of the transcription activity of Epstein-Barr virus nuclear antigen 2 and also as a protein that is essential for normal growth of B lymphocytes.[2] SND1 has four staphylococcal nuclease-like domains (SN-like domains) and a Tudor domain.[15] It has been demonstrated to bind with signal transducer and activator of transcription 6 via an SN-like domain, to bind with the large fragment of RNA polymerase II, and to control the basal transcription mechanism of signal transducer and activator of transcription 6 by a bridging function.[16] In addition, SND1 binds to c-Myb, a differentiation and growth factor of immature hematopoietic cells and lymphocytes, suggesting involvement in up-regulation of translation.[17] Although SND1 is located primarily in the cytoplasm, it can also migrate to the nucleus and has been indicated as possessing the potential to control translation activity.[18] Tsuchiya et al[19] reported the involvement of SND1 in colon carcinogenesis, with SND1 suppressing the adenomatous polyposis coli protein level via a post-transcriptional mechanism. These authors found no relation to tumor aggressiveness or progression, leading them to suggest possible involvement of SND1 in early-stage carcinogenesis in colon cancer. In prostate cancer, although SND1 could contribute to the RNA degradation observed in RNA interference, the target RNA has not been defined. However, many miRs were up-regulated in prostate cancer, and targets of these miRs include major tumor suppressor genes. For example, let-7 negatively regulates Ras, miR-17-5p, and miR-20a control E2F, and miR-16-1 and miR-15a repress Bcl-2.[5] Since the miR machinery including engagement of SND1 in prostate cancer is somewhat of a black box, further studies are warranted.

In conclusion, SND1 may have the potential for identification of the more aggressive and clinically significant prostate cancers.

Acknowledgments

References

1. Kuruma H, Egawa S, Oh-Ishi M, Kodera Y, Satoh M, Chen W, Okusa H, Matsumoto K, Maeda T, Baba S: High molecular mass proteome of androgen-independent prostate cancer. Proteomics 2005, 5:1097–1112
2. Tong X, Drapkin R, Yalamanchili R, Mosialos G, Kieff E: The Epstein-Barr virus nuclear protein 2 acidic domain forms a complex with a novel cellular coactivator that can interact with TFIIE. Mol Cell Biol 1995, 15:4735–4744
3. Bernstein E, Caudy AA, Hammond SM, Hannon GJ: Role for a bidentate ribonuclease in the initiation step of RNA interference. Nature 2001, 409:363–366

4. Volinia S, Calin GA, Liu CG, Ambs S, Cimmino A, Petrocca F, Visone R, Iorio M, Roldo C, Ferracin M, Prueitt RL, Yanaihara N, Lanza G, Scarpa A, Vecchione A, Negrini M, Harris CC, Croce CM: A microRNA expression signature of human solid tumors defines cancer gene targets. Proc Natl Acad Sci USA 2006, 103:2257–2261

5. Chiosea S, Jelezcova E, Chandran U, Acquafondata M, McHale T, Sobol RW, Dhir R: Up-regulation of dicer, a component of the MicroRNA machinery, in prostate adenocarcinoma. Am J Pathol 2006, 169:1812–1820

6. Magi-Galluzzi C, Luo J, Isaacs WB, Hicks JL, de Marzo AM, Epstein JI: Alpha-methylacyl-CoA racemase: a variably sensitive immunohistochemical marker for the diagnosis of small prostate cancer foci on needle biopsy. Am J Surg Pathol 2003, 27:1128–1133

7. Gleason DF: Classification of prostatic carcinomas. Cancer Chemother Rep 1966, 50:125–128

8. UICC International Union: UICC International Union Against Cancer, TNM classification of malignant tumors, 6th ed. Edited by Sobin LH, Wittekind CH. New York, John Wiley & Sons, Inc, 2002, pp. 184–187

9. Tsuchiya B, Sato Y, Montone KT, Nagai T, Kameya T: Four-hour double staining for in situ hybridization and immunohistochemistry. The J Histotechnol 2000, 23:321–325

10. Rubin MA, Zhou M, Dhanasekaran SM, Varambally S, Barrette TR, Sanda MG, Pienta KJ, Ghosh D, Chinnaiyan AM: alpha-Methylacyl coenzyme A racemase as a tissue biomarker for prostate cancer. JAMA 2002, 287:1662–1670

11. Humphrey PA: Diagnosis of adenocarcinoma in prostate needle biopsy tissue. J Clin Pathol 2007, 60:35–42

12. Epstein JI, Partin AW, Sauvageot J, Walsh PC: Prediction of progression following radical prostatectomy. A multivariate analysis of 721 men with long-term follow-up Am J Surg Pathol 1996, 20:286–292

13. Steinberg DM, Sauvageot J, Piantadosi S, Epstein JI: Correlation of prostate needle biopsy and radical prostatectomy Gleason grade in academic and community settings. Am J Surg Pathol 1997, 21:566–576

14. Montironi R, Mazzuccheli R, Scarpelli M, Lopez-Beltran A, Fellegara G, Algaba F: Gleason grading of prostate cancer in needle biopsies or radical prostatectomy specimens: contemporary approach, current clinical significance and sources of pathology discrepancies. BJU Int 2005, 95:1146–1152

15. Callebaut I, Mornon JP: The human EBNA-2 coactivator p100: multidomain organization and relationship to the staphylococcal nuclease fold and to the tudor protein involved in Drosophila melanogaster development. Biochem J 1997, 321:125–132

16. Yang J, Aittomäki S, Pesu M, Carter K, Saarinen J, Kalkkinen N, Kieff E, Silvennoinen O: Identification of p100 as a coactivator for STAT6 that bridges STAT6 with RNA polymerase II. EMBO J 2002, 21:4950–4958

17. Leverson JD, Koskinen PJ, Orrico FC, Rainio EM, Jalkanen KJ, Dash AB, Eisenman RN, Ness SA: Pim-1 kinase and p100 cooperate to enhance c-Myb activity. Mol Cell 1998, 2:417–425

18. Ness SA: Myb binding proteins: regulators and cohorts in transformation. Oncogene 1999, 18:3039–3046

19. Tsuchiya N, Ochiai M, Nakashima K, Ubagai T, Sugimura T, Nakagama H: SND1, a component of RNA-induced silencing complex, is up-regulated in human colon cancers and implicated in early stage colon carcinogenesis. Cancer Res 2007, 67:9568–9576

Identification of peptides applicable as vaccines for HLA-A26-positive cancer patients

Yamei Niu,[1,3] Yasunobu Terasaki,[1] Nobukazu Komatsu,[1] Masanori Noguchi,[2] Shigeki Shichijo[1,4] and Kyogo Itoh[1]

Departments of [1]Immunology and Immunotherapy and [2]Urology, Kurume University School of Medicine, Kurume, Fukuoka, Japan; [3]Genome Stability Group, Beijing Institute of Genome, Chinese Academy of Science, Beijing, China

One-fifth of the Japanese population is positive for HLA-A26, but few peptides are available as potential cancer vaccines for HLA-A26-positive cancer patients. The objective of this study was to identify peptide vaccine candidates for HLA-A26-positive cancer patients. The HLA-A*2601-crossbinding activity of 24 peptides currently under clinical trial as vaccines for HLA-A2, -A24, or HLA-A3 supertype-positive cancer patients was evaluated by stabilization assay. Three peptides with HLA-A2-binding activity could bind the HLA-A*2601 molecule. These three peptides induced HLA-A26-restricted cytotoxic T lymphocytes from HLA-A*2601-, -A*2602-, or -A*2603-positive prostate cancer patients against HLA-A*2601- and HLA-A*2603-positive cancer cells in CD8-dependent and peptide-specific manners. In addition, one peptide with HLA-A24-binding activity could bind to HLA-A*2601 and induced HLA-A26-restricted cytotoxic T lymphocytes from HLA-A*2601-, -A*2602-, or -A*2603-positive prostate cancer patients against HLA-A*2603-positive cancer cells. These results may provide novel information for the development of a peptide-based cancer vaccine for HLA-A26-positive patients. (*Cancer Sci* 2009; 100: 2167–2174)

P eptide vaccines have gained more attention in recent years as potentially efficient and safe therapeutic modalities against cancer and viral diseases. So far, most studies investigating epitope-based cancer vaccines have focused on HLA-A2, -A24, and -A3 supertype molecules due to their high frequencies in worldwide populations. In contrast, HLA-A26-restricted peptides vaccines have not been studied comprehensively even though HLA-A26 is present as phenotype in 21% of the Japanese population.[1] The HLA-A26 allele is found in approximately 11% of the Japanese population, 4% of the Caucasian population in the USA, and 7.5% of the African population of Cape Town, South Africa.

Recently, we reported that certain peptides could bind more than one type of HLA molecule and induce related cytotoxic T lymphocyte (CTL) responses.[2,3] Therefore, this study aimed to determine whether peptides currently under clinical trial as vaccines for HLA-A2, -A24, and HLA-A3 supertype–positive cancer patients could be applicable in HLA-A26-positive patients.

Materials and Methods

Patients and samples. The Institutional Ethical Review Board of Kurume University approved the study protocol, which conformed to the ethical guidelines of the 1975 Declaration of Helsinki. Informed written consent was obtained from all participants who donated PBMCs for this study. Patients with prostate cancer who provided PBMCs for this study were patients (Pt.) 71, HLA-A*2601/A*2602; Pt. 75, A*2602/A*2602; Pt. 102, A*2402/A*2603; Pt. 125, A*2402/A*2601; and Pt. 137, A*2402/A*2602. None of the participants was infected with human immunodeficiency virus (HIV), hepatitis B virus, or hepatitis C virus (HCV). Twenty mL of peripheral blood was obtained from each participant, and PBMCs were prepared by the Ficoll-Conray density centrifugation method. The expression of HLA molecules on the PBMCs was determined by flow cytometry analysis using the EPICS-XL (Beckman Dickinson, Mountain View, CA, USA). All samples were cryopreserved until the experiments were performed.

Antibodies. Anti-HLA-A2 monoclonal antibody (mAb) was prepared from hybridoma clone BB7.2 (ATCC, Rockville, MD, USA). Anti-HLA-A24 mAb (cat. no.0041HA), anti-HLA-A11 mAb (cat. no. 0284HA), anti-HLA-A26 mAb (cat. no. 0514AHA), anti-HLA-A31 mAb (cat. no. 0273HA), and anti-HLA-A33 mAb (cat. no. 0612HA) were purchased from One Lambda (Canoga, CA, USA). Anti-MHC class I (W6/32) was obtained from Dako (cat. no. M0736; Glostrup, Denmark). Fluorescein (FITC)-conjugated goat IgG antimouse IgG was purchased from Cappel (cat. no. 55493; Aurora, OH, USA), and FITC-conjugated goat antimouse IgM was purchased from Bioscource (Camarillo, CA, USA). Anti-CD4 (Nu-Th/T), -CD8 (Nu-Ts/c), -CD14 (JML-H14), and -MHC class II (H-DR-1) Abs were purified from ascites of mice immunized with the corresponding hybridoma. Anti-HLA-B, -C Ab (B1-23, IgG2a) was kindly donated by Dr. Pierre G. Coulie (Catholic University of Louvain, Brussels, Belgium). Mouse anti-hnRPL mAb was purchased from Abcam (clone 4D11, ab6101; Tokyo, Japan). Mouse anti-WNK2 (46.21) mAb (sc-100452) and rabbit anti-NELF-A (H-240) (Ab to WHSC2) (sc-32911) were purchased from Santa Cruz Biotechnology (Santa Cruz, CA, USA).

Cell lines. RMA-S cells (mouse lymphoma cell line deficient in transporter associated with antigen processing [TAP]) were maintained in RPMI-1640 supplemented with 10% FCS. RMA-S-A*2601/human beta-2-microglobulin (hb2m) cells were established as described previously[2] and maintained in RPMI-1640 supplemented with 10% FCS, 0.75 mg/mL of Geneticin (Calbiochem, Darmstadt, Germany), and 2 μg/mL of Puromycin (Calbiochem).

KNS-42 (HLA-A*2402/A*2601, malignant glioma cell line) and BECHER (HLA-A*6802/A*0301, astrocytoma cell line) cells were cultured in Eagle's Minimal Essential Medium supplemented with 10% FCS. KNS-81 (HLA-A*2402/–, malignant glioma cell line) and ONS-76 (HLA-A*2402/A*2603, medulloblastoma cell line) cells were cultured in DMEM supplemented with 10% FCS. KINGS-1 (HLA-A*2601/A*3101, anaplastic astrocytoma cell line) were cultured in RPMI-1640 supplemented with 10% FCS.

Peptides. Peptides were purchased from Multiple Peptide Systems (purity >99.5%; San Diego, CA, USA) or Thermo Fisher Scientific (purity >90%; Waltham, MA, USA). All peptides were dissolved in DMSO to a final concentration of 10 mg/mL and stored at −80°C prior to use. Details are shown in Table 1.

[4]To whom correspondence should be addressed.
E-mail: shichijo@med.kurume-u.ac.jp

Table 1. Peptides used in this study and their HLA-A*2601 binding data

HLA type	Peptide	Sequence	Binding score†	MFI increase (%)‡
A2	§HCV C35-44	YLLPRRGPRL	10	150
	SART3 302-310	LLQAEAPRL	8	105
	HNRPL 501-510	NVLHFFNAPL	18	135
	ppMAPkkk 432-440	DLLSHAFFA	9	121
	UBE 43-51	RLQEWCSVI	3	103
	Lck 246-254	KLVERLGAA	12	100
	CypB 129-138	KLKHYGPGWV	1	107
	Lck 422-430	DVWSFGILL	29	110
	WHSC2 103-111	ASLDSDPWV	4	114
A24	SART3 109-118	VYDYNCHVDL	8	123
	PAP 213-221	LYCESVHNF	14	100
	Lck 208-216	HYTNASDGL	9	110
	SART2 93-101	DYSARWNEI	8	101
	Lck 488-497	DYLRSVLEDF	20	100
	MRP2 1293-1302	NYSVRYRPGL	8	100
	PSA 248-257	HYRKWIKDTI	1	100
	EGFR 800-809	DYVREHKDNI	12	96
A3	§HCV C30-39	IVGGVYLLPR	15	100
	Lck 449-458	VIQNLERGYR	5	100
	SART3 511-519	WLEYYNLER	1	100
	Lck 90-99	ILEQSGEWWK	0	95
	IEX 47-56	APAGRPSASR	1	100
	PSA 16-24	GAAPLILSR	8	100
	SART3 734-42	QIRPIFSNR	8	100
	β-tubulin5 154-162	KIREEYPDR	1	100
	PAP 248-257	GIHKOKEKSR	5	100
A26	§HCV NS3 1582-1590	ENLPYLVAY	26	140

†Binding score: calculation based on SYFPEITHI database (http://www.syfpeithi.de/). ‡MFI increase: ratio between MFI of peptide treated sample and DMSO treated sample at 100 μM. §Peptides that are used as control in the experiments.

Stabilization assay. Binding activities of each peptide to HLA-A*2601 were examined by means of stabilization assay as previously reported.[4] Briefly, RMA-S-A*2601/hb2m cells cultured at 26°C overnight in RPMI-1640 medium were incubated at 26°C for 3 h then 37°C for 2 h in OPTI-MEM (Invitrogen, Carlsbad, CA, USA) containing 4 μg/mL hb2m (CP1022; Fitzgerald, Concord, MA, USA) and peptides at 1 μM, 10 μM, or 100 μM. Cells were harvested and washed with PBS once. HLA-A*2601 molecules on cell surfaces were stained with mouse anti-HLA-A26 and FITC-conjugated antimouse IgM, and then analyzed using the EPICS XL. The affinities of the peptides to HLA molecules were evaluated by the percent mean fluorescence intensity (MFI %) increase of the HLA molecules detected by staining with the specific mAb using the following calculation: MFI increase % = [(MFI induced by peptide − MFI induced by DMSO)/(MFI induced by DMSO)] × 100%.

⁵¹Cr-release assay. The cytotoxicity of peptide-stimulated PBMCs was measured by ⁵¹Cr-release assay.[4] PBMCs (1 × 10⁵ cells/well) were incubated with 10 μM of each peptide in a U-bottom-type 96-well micro-culture plate in 200 μL of culture medium (45% RPMI-1640, 45% AIM-V medium, 10% FCS, 100 U/mL of interleukin [IL]-2, 0.1 mM MEM nonessential amino acid solution). Every 3 to 4 days, half of the culture medium was replaced with new medium containing the corresponding peptide (20 μM). After five cycles of peptide pulse, cells were cultured for another 1–2 weeks in culture medium only. KNS-42 (HLA-A*2402/A*2601), KINGS-1 (HLA-A*2601/A*3101), or ONS-76 (HLA-A*2402/A*2603) cells were used as positive target cells in each assay; KNS-81 (HLA-A*2402/−) or BECHER (HLA-A*6801/A*0301) cells were

used as negative target cells. Protein expression levels of heterogeneous nuclear ribonucleoprotein L (HNRPL),[5] with no Lysine (K) 2 (WNK2, ppMAPkkk),[6] and Wolf–Hirschhorn syndrome candidate 2 (WHSC2, also known as NELF-A)[7] were detected using the Leucoperm kit (AbD Serotec, Oxford, UK) and corresponding antibodies, according to the data sheet. Phytohemagglutinin (PHA)-activated T-cells were used as negative control cells. Two thousand ⁵¹Cr-labeled target cells per well were cultured in a 96-well plate with effector cells at the indicated effector to target cell (E/T) ratios. The specific ⁵¹Cr-release was calculated according to the following formula: % specific lysis = (test sample release − spontaneous release) × 100/(maximum release spontaneous release). Maximum release was determined from the supernatant of the sample incubated in 1% Triton-X (Wako Pure Chemical Industries, Osaka, Japan); spontaneous release was determined from the supernatant of the sample incubated with medium only.

Blocking inhibition assay and cold competition assay. The HLA specificity of the cytotoxicity of peptide-stimulated PBMCs was confirmed by blocking inhibition assay. Before ⁵¹Cr-release assay, effector cells were treated with anti-CD4, anti-CD8, or anti-CD14 antibodies at a final concentration of 20 μg/mL; radiolabeled target cells were treated with anti-HLA class I (W6/32), anti-HLA class II, or anti-HLA-B, C Abs. After Ab blocking for 1–2 h, ⁵¹Cr-release assay was performed at the indicated E/T ratio.

Cold competition assay was performed to confirm the peptide specificity of peptide-induced cytotoxicity. Immediately before the assay, C1R-A*2601 cells were incubated with 10 μM of peptide (C35-44 peptide or HIV-A26 peptide as a negative control) at 37°C for 2 h, and then 2 × 10⁴ peptide-pulsed cells were added to each well containing target cells and effector cells as cold target cells. After a 6-h incubation, cytotoxicity was measured as described above.

Results

Binding activity. Eight peptides were selected from each group of peptides previously identified based on their HLA-A2, -A24,[8] or HLA-A3[9,10] supertype restriction; thus, 24 peptides were examined for binding activity to HLA-A*2601 molecules. Initially, binding scores of these peptides were calculated based on motifs obtained from SYFPEITHI database (Table 1).[11] Actual binding affinities of these peptides for HLA-A*2601 molecules were evaluated via stabilization assay. HCV NS3 1582-1590[12] was used as a positive control; DMSO and HCV C30-39[12] were used as negative controls. Three HLA-A2-binding peptides (ppMAPkkk 432-440, HNRPL 501-510, and WHSC2 103-111)[7] and one HLA-A24-binding peptide (SART3 109-118)[3,13] were selected based on their relatively higher MFI increases at 100 μM relative to the other 20 peptides (Table 1). In contrast to HLA-A2 and -A24 typed peptides, no HLA-A3-supertype binding peptide bound to HLA-A*2601. These four peptides were further assayed at concentrations of 1, 10, and 100 μM. All four peptides stabilized HLA-A*2601 expression on the cell surface in a dose-dependent manner (Fig. 1).

Expression of antigens on target cells. Expression of HLA-A26 molecules and the tumor antigens HNRPL, WNK2 (ppMAPkkk), and WHSC2 (NELF A) in the target cancer cells used for the cytotoxicity assay was investigated by flow cytometry analysis. As expected from previous results,[7] all of these molecules were expressed in the cancer cells; representative results are shown in Figure 2. However, these antigens were not detected in PHA-activated T-cells using same method (data not shown). According to SART3 antigen, we previously reported the ubiquitously expression in cancer cell lines[3,13,14] including KINGS-1, ONS-81, KNS-42, and BECHER but not in PBMC.
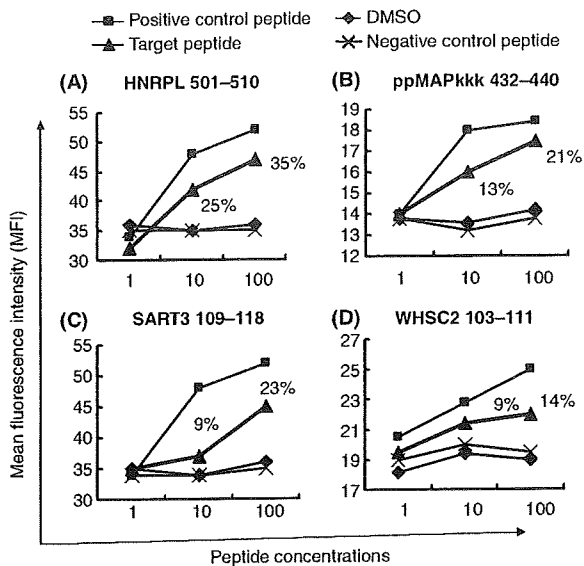
Fig. 1. Stabilization analysis of peptide binding to HLA-A*2601 molecules. Binding activities of HNRPL 501-510 (A), ppMAPkkk 432-440 (B), SART3 109-110 (C), and WHSC2 103-111 (D) were examined using RMA-S cells stably expressing HLA-A*2601 and hb2m. A positive control (hepatitis C virus [HCV] NS3 1582-1590), negative control (HCV C30-39), and DMSO control were included in each assay. Mean fluorescence intensity (MFI) increases were recorded at 1, 10, and 100 μM of the peptides or DMSO. The MFI increase induced by each peptide relative to that for DMSO was calculated and is shown in each figure. Representative results from at least three experiments are shown.
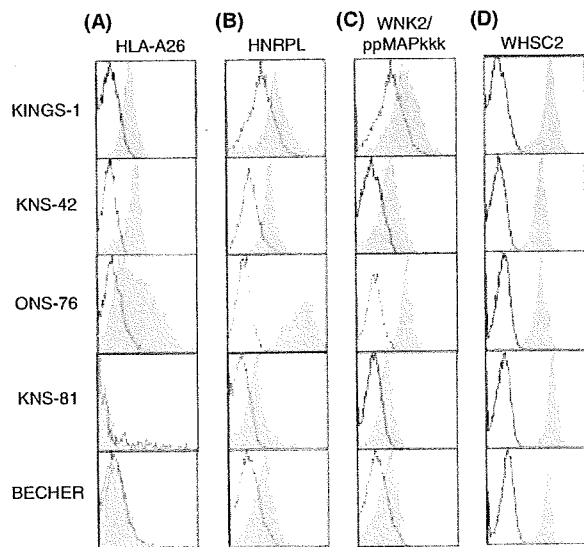
Fig. 2. Protein expression profiles of HLA-A26 and the four cancer antigens in target cells used for ^{51}Cr-release assay. (A) Cells were washed with PBS and then stained with the corresponding antibodies (Abs). (B–D) Cells were washed with PBS once, fixed and permeabilized using Leucoperm, and then stained with the corresponding Abs. Flow cytometry analysis was performed using EPICS-XL. Black lined peaks indicate negative control without primary Ab; grey peaks indicate the protein expression profiles of target molecules.

Induction of cytotoxic T lymphocytes by HLA-A2-binding peptides. Initially, we tested the capability of three of the HLA-A2-binding peptides (ppMAPkkk 432-440, HNRPL 501-510, and WHSC2 103-111) to induce CTLs. Peptide-induced CTLs from Pt. 125 (HLA-A*2402/A*2601), which were prepared by *in vitro* incubation of the PBMCs with each of the three peptides, showed dose-dependent cytotoxicity against HLA-A*2601-positive cancer cells (KNS-42), but not against negative cancer cell lines (KNS-81 or BECHER), as HLA-A26-negative and antigen-positive controls, or against PHA-activated T-cells, as HLA-A26-positive and antigen-negative controls. Representative results are shown in the left panels of Figure 3(A). In order to determine whether there was cross reactivity among different HLA-A26 subtypes, we performed similar experiments using HLA-A*2603-positive cancer cells (ONS-76) as target cells. As shown in the right panels of Figure 3(A), all peptide-induced HLA-A*2601-restricted CTLs from Pt. 125 showed dose-dependent cytotoxicity against ONS-76 cells. CTL activity against HLA-A*2602-positive cancer cells was not tested since such these cancer cells were not available.

Similar CTL activity was obtained from HLA-A*2602-positive and HLA-A*2603-positive PBMCs from cancer Pts. 137 and 102. Representative results are shown in Figures 3(B) and 2(c), respectively. HLA-A24-negative and -A26-positive KINGS-1 cells were used as target cells in Figures 3(B) and 2(c) (both left). These CTLs failed to exhibit cytotoxicity against HLA-A24-positive KNS-81 target cells used as negative control cells. There was no significant difference in the degree of cytotoxicity against HLA-A*2601-positive cancer cells and that against HLA-A*2603-positive cancer cells.

HLA specificity was examined via Ab blocking inhibition. CTL activity of peptide-induced HLA-A*2601-restricted CTLs from Pt. 125 against HLA-A*2601-positive target cells was suppressed significantly by both anti-CD8 Ab and anti-HLA class I Ab (Fig. 4A), indicating that the cytotoxicity mediated by these peptides was HLA class I restricted and CD8$^+$ T-cell dependent. Similar results were obtained using HLA-A*2602-positive (Pt. 137) and -A*2603-positive (Pt. 102) PBMCs; these peptide-specific CTL cytotoxicities were also HLA class I and CD8 restricted (Fig. 4B,C).

In addition, cytotoxicity against target cells was significantly suppressed by the addition of corresponding peptide-pulsed unlabeled C1R-A*2601 cells, but not by HIV peptide-pulsed unlabeled C1R-A*2601 cells (Fig. 5). These results indicate that the cytotoxicity of peptide-induced CTLs against cancer cells could be ascribed to the corresponding peptide-specific CD8$^+$ T-cells.

Induction of CTLs by HLA-A24-bound peptides. We tested the ability of one of the HLA-A24-binding peptides (SART3 109-118, VYDYNCHVDL) to induce CTLs using PBMCs from Pt. 71 (HLA-A*2601/A*2602), Pt. 75 (HLA-A*2602/A*2602), and Pt. 102 (HLA-A*2402/A*2603) as effector cells. Cancer cell lines used as target cells were KINGS-1 (HLA-A*2601/A*3102), KNS-42 (HLA-A*2402/A*2601), and KNA-81 (HLA-A*2402/–). PHA-blast cells (HLA-A*0201/A*2601) were used as negative control cells. In Pt. 71 (HLA-A*2601/A*2602), SART3 109-118 induced CTL activity against KINGS-1(HLA-A*2601/A*3102) but not KNA-81 (HLA-A*2402/–) or PHA-blast cells (Fig. 6A).

SART3 109-118 also induced CTL activity against KNS-42 (HLA-A*2402/A*2601) in Pt. 75 (HLA-A*2602/A*2602), but not against KNA-81 (HLA-A*2402/–) or PHA-blast cells (HLA-A*2602; Fig. 6A). Neither MHC restriction nor cold target competition assay was conducted because there were insufficient effector cells for such assays.

The CTLs from Pt. 102 (A*2402/A*2603) showed cyotoxicity against KINGS-1 (A*2601/A*3102) and no cytotoxicity

Niu et al.

131
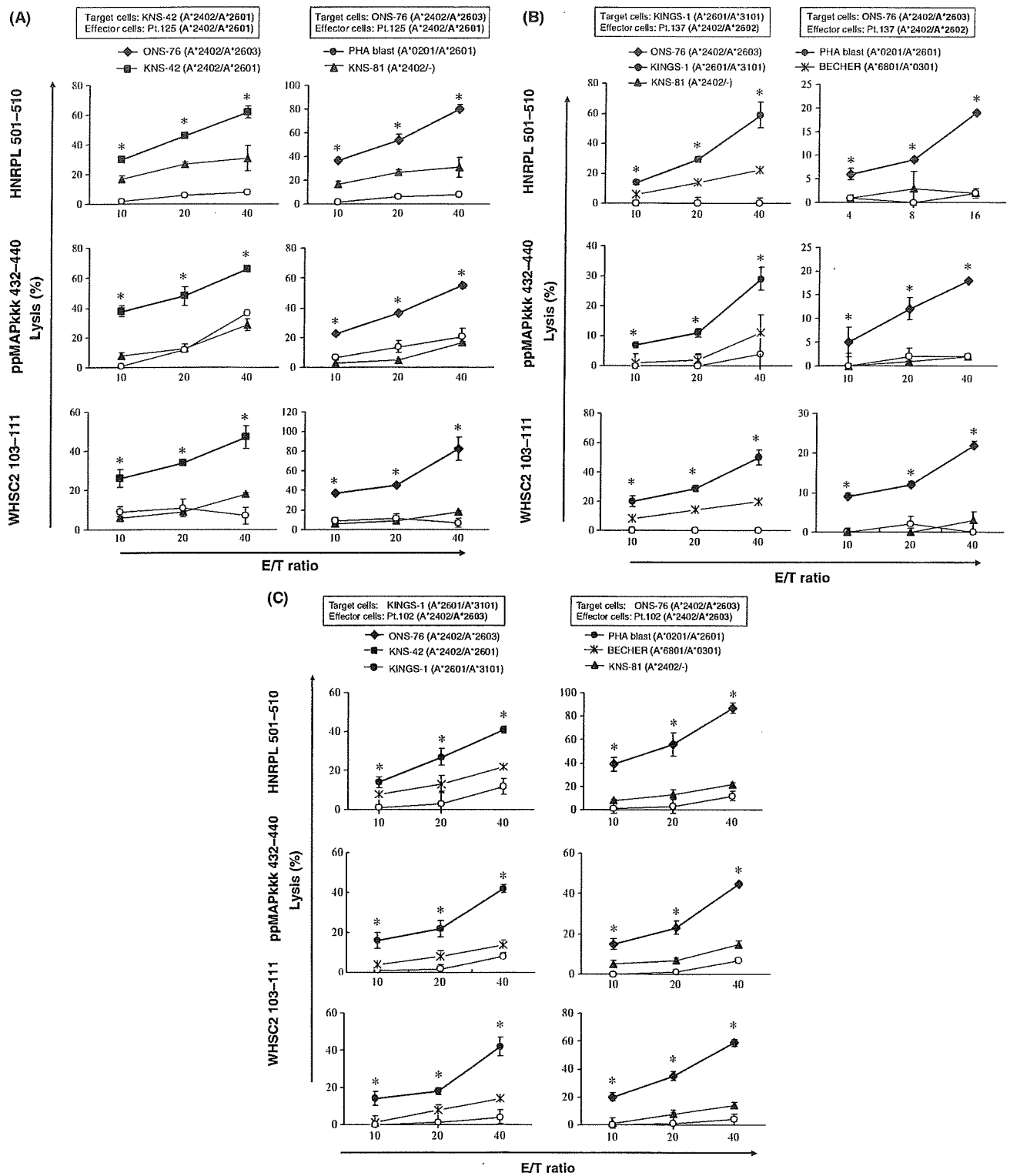
Fig. 3. Cytotoxicities of peptide-induced cytotoxic T lymphocytes (CTLs) generated *in vitro* from PBMCs of HLA-A26-positive prostate cancer patients. Peptide-induced CTLs from (A) Pt. 125 (HLA-A*2402/A*2601), (B) Pt. 137 (HLA-A*2402/A*2602), and (C) Pt. 102 (HLA-A*2402/A*2603) were tested for cytotoxicity at effector to target cell (E/T) ratios of 10, 20, and 40 by ^{51}Cr-release assay against KINGS-1 (HLA-A*2601/A*3101), KNS-42 (HLA-A*2402/A*2601), or ONS-76 (HLA- A*2402/A*2603) cells. HLA-A26-positive phytohemagglutinin (PHA)-activated T-cells and HLA-A-26-negative cancer cells, including BECHER and KNS-81, were used as negative controls in each experiment. Experiments were performed in triplicate and repeated at least twice. Representative results are shown. Statistical analysis was performed by two-tailed student's *t*-test (*$P < 0.05$).
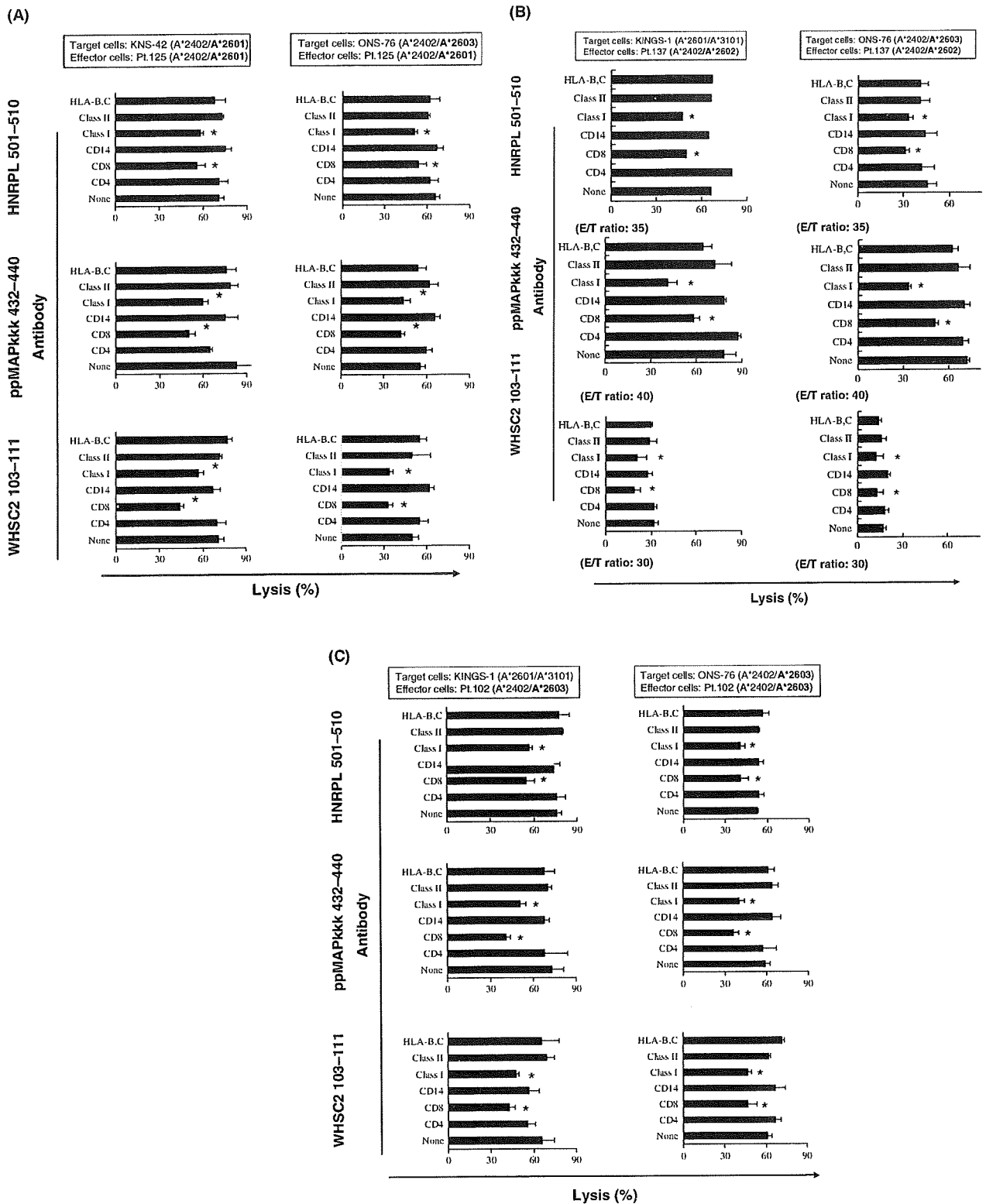
132

Fig. 4. HLA specificity of peptide-induced cytotoxic T lymphocyte (CTL) cytotoxicity. Peptide-induced CTLs from (A) Pt. 125 (HLA-A*2402/A*2601), (B) Pt. 137 (HLA-A2402/A*2602), and (C) Pt. 102 (HLA-A*2402/A*2603) were treated with 20 μg/mL anti-CD4, anti-CD8, or anti-CD14 mAb; HLA-A*2601-positive (left panel) or HLA-A*2603-positive (right panel) target cancer cells were treated with 20 μg/mL anti-MHC class I, anti-MHC class II, or anti-HLA-B, C mAb. ^{51}Cr-release assay was performed as described above at an effector to target cell (E/T) ratio of 40 or at the indicated E/T ratio. Statistical analysis was performed by two-tailed Student's t-test (*$P < 0.05$).
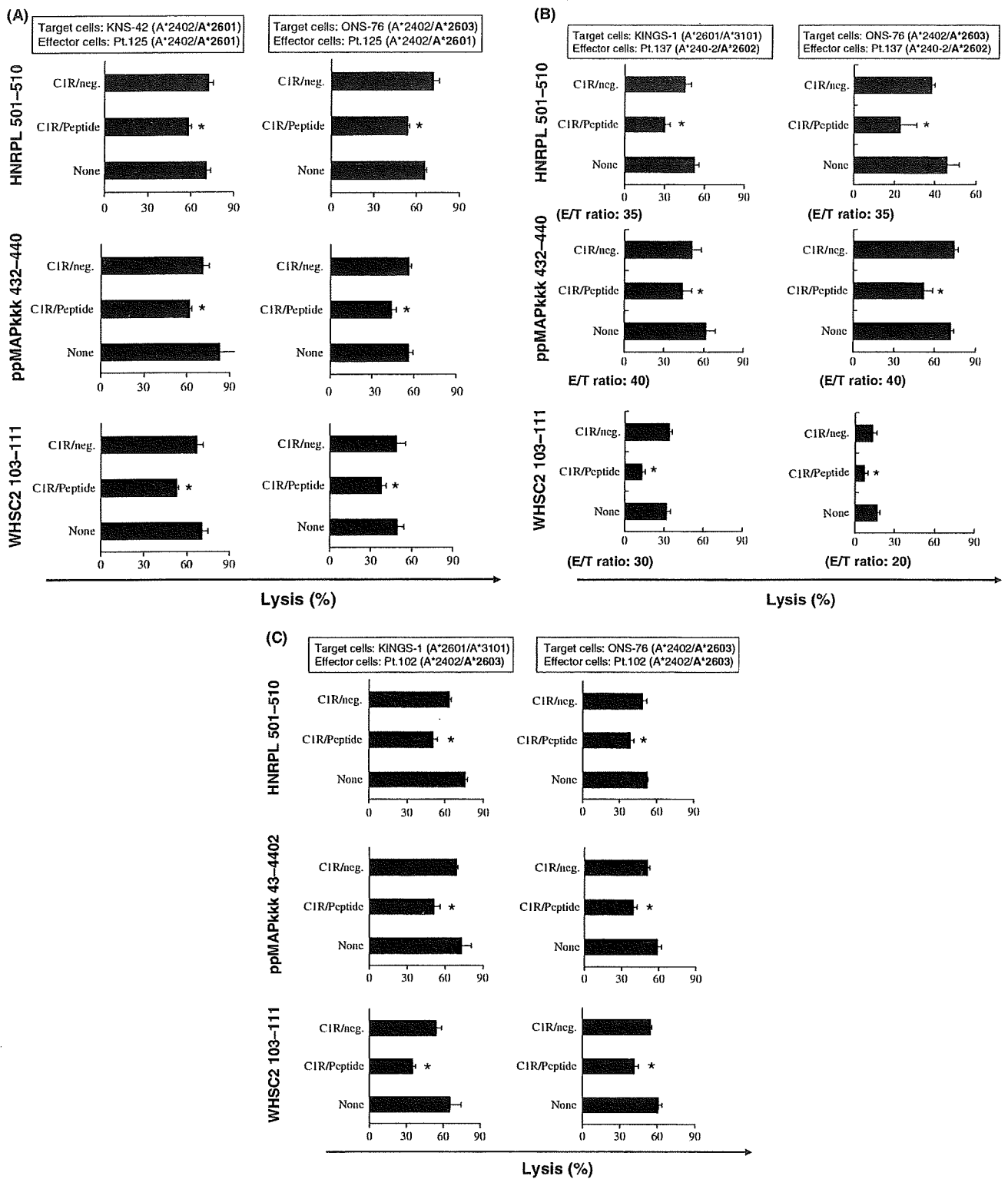
Niu *et al.*

Fig. 5. Peptide-specificity of cytotoxic T lymphocyte (CTL) cytotoxicity. Peptide-induced CTLs from (A) Pt. 125 (HLA-A*2402/A*2601), (B) Pt. 137 (HLA-A2402/A*2602), and (C) Pt. 102 (HLA-A*2402/A*2603) were tested for their cytotoxicity against corresponding target cells in the presence or absence of unlabeled C1R-A*2601 cells (C1R/peptide and C1R/neg., respectively), which were preloaded with either the corresponding peptide or the HCV C35-44 peptide. ^{51}Cr-release assay was performed as described above at an effector to target cell (E/T) ratio of 40 or at the indicated E/T ratio. Statistical analysis was performed by a two-tailed Student's t-test ($*P < 0.05$) as compared to the data for no cold target samples (none).

134
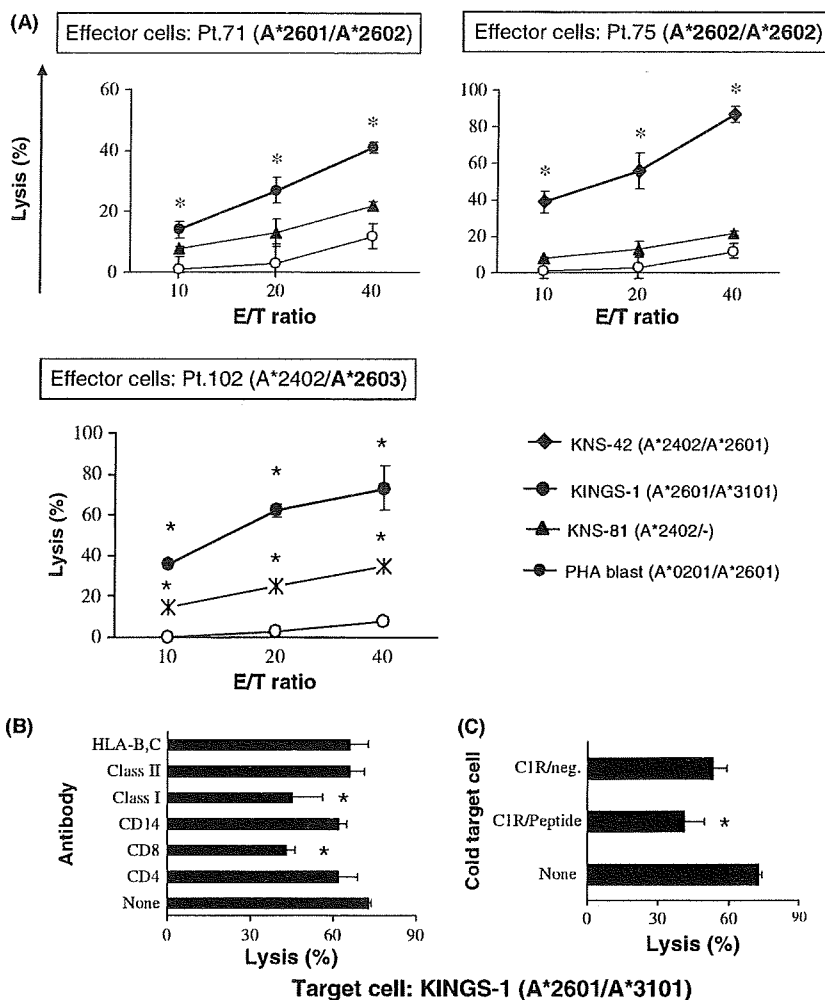
Fig. 6. Cytotoxic activity and MHC-restriction and peptide specificities of SART3 109-118-induced CTLs. (A) Cytotoxicities of SART3 109-118-induced CTLs generated *in vitro* (Pt. 71, HLA-A*2601/A*2602; Pt. 75, HLA-A*2602/A*2602; Pt. 102, HLA-A*2402/A*2602). CTLs were tested for cytotoxicity at effector to target cell (E/T) ratios of 10, 20, and 40 by ^{51}Cr-release assay against KNS-42 cells for Pt. 71 and Pt. 75, and KINGS-1 for Pt. 102. HLA-A26-positive phytohemagglutinin (PHA)-activated T-cells and HLA-A-26-negative KNS-81 cancer cells were used as negative controls in each experiment. (B) HLA specificity of SART3 109-118-induced CTL cytotoxicity for Pt. 102. The method was the same as described for Figure 4. (C) SART3-109-specificity of CTL cytotoxicity for Pt. 102. The method was the same as described for Figure 5. Experiments were performed in triplicate and repeated at least twice. Representative results shown here. Statistical analysis was performed by a two-tailed student's t-test ($*P < 0.05$).

against PHA-blast cells (Fig. 6A). MHC restriction and peptide specificity were confirmed by inhibition assays (Fig. 6B,C). These results indicate that SART3-109, with an HLA-A24 binding motif, could induce CTLs against HLA-A*2601-positive cancer cells in patients positive for HLA-A*2602 and A*2603, probably in MHC-restricted and peptide-specific manners.

Discussion

Historically, it has been accepted that peptides bind to MHC molecules with strict specificity. However, several recent studies have revealed that this strictness is less than absolute.[3,15–17] Results from our previous study indicated that a certain few peptides could bind to more than one type of HLA molecule.[2,3,18]

In silico analysis has been utilized widely to identify novel vaccine epitopes; in this study, the SYFPEITHI database was used to pre-analyze the binding scores of each peptide of interest to HLA-A*2601. However, analysis of the results for some known peptides indicated that the SYFPEITHI binding scores did not always correlate with the real binding affinities of the peptides to the corresponding HLA molecule.[2,3,19] Therefore, stabilization assays were performed to confirm binding activity. Thusly, four of the 24 peptides identified according to their abilities to bind other HLA molecules could also bind HLA-A*2601, supporting the hypothesis that certain peptides can bind multiple HLA types.

In addition to *in vitro* binding ability, these four peptides also induced HLA-A26-restricted CTLs that showed cytotoxicity against HLA-A26-positive but not HLA-A26-negative cancer cells. Although the binding affinity of the WHSC2 103-110 peptide was weaker than that of the remaining three peptides (Fig. 1), no significant difference was observed among their abilities to induce CTLs. The binding abilities of the peptides with HLA-A*2602 and -A*2603 were not examined because these two molecules were not available.

HLA-A*2601 is highly homologous to HLA-A*2602 and -A*2603. Therefore, our results showing that the four peptides could induce CTLs against HLA-A*2603-positive cancer cells in HLA-A*2602 and -A *2603 patients were expected. Because HLA-A*2602-positive cancer cells were not available for research purposes, only HLA-A*2601-positive and HLA-A*2603-positive cancer cells were used as target cells for all three HLA-A26-restricted CTLs in the ^{51}Cr-release assay. Previously, it was reported that peptide-induced HLA-A*2601-restricted CTLs were cytotoxic only against HLA-A*2601-positive cancer cells but not against HLA-A*2603-positive cancer cells.[2,20] However, in our studies, all four peptide-induced CTLs showed similar cytotoxicity against HLA-A*2601-positive and -A*2603-positive cancer cells. These discrepancies could have resulted from at least three factors. First, different peptides could have different abilities to react with one or more types of HLA molecule. Out of 24 peptides, these four peptides

Niu et al.

135

were found to bind HLA-A2 (or HLA-A24) and HLA-A26; therefore, it is not surprising that they could bind to all the three HLA-A26 subtype alleles. Not all peptides have this ability. Second, in our experience, different cancer cell lines have different sensitivities to activated CTLs even when they have the same HLA-A26 alleles. Third, expression levels of cancer antigens by the target cells might also affect the level of observed cytotoxicity. In this study, only HLA-A26-positive cells that expressed a sufficient amount of cancer antigen were used as positive target cells. However, expression of cancer antigen in target cells was not examined in previous studies. Therefore, further studies are necessary to examine the interaction between HLA-A26-restricted CTLs and cancer cells. In addition, stabilization assays are necessary to determine the binding affinities between these peptides and HLA-A*2602 and -A*2603 once the corresponding cDNA has been obtained.

It is known that the main binding energy in HLA class I activity is provided by the interaction between residues in position 2 and the C-terminus of the peptide and the B- and F-binding pockets of the MHC molecules, although side chains throughout the ligand can positively or negatively influence binding capacity. For the B-pocket structure, residues 9, 45, 63, 66, 67, 70, and 99 are key residues, which include 'YMNNVHY' for HLA-A*2601-3. For the F pocket, the key residues are those in positions 77, 80, 81, and 116, which include 'NTLD' for HLA-A*2601 and 'NTLN' for HLA-A*2602; no information is yet available for HLA-A*2603. According to homology analysis of the three HLA-A26 alleles, there is no difference between HLA-A*2601 and HLA-A*2602 molecules except at amino acid position 116. In contrast, there are differences between HLA-A*2601 and HLA-A*2603 at positions 74, 76, and 77. Therefore, these three subtypes have the same B-pocket structure and only one amino acid difference in the F-pocket structure. This could explain why HLA-A*2601-, -A*2602-, and -A*2603-

restricted CTLs could all be induced by the four different peptides.

Previously, it was reported that CTLs could not be induced against high HLA-A2-binding peptides possibly because of tolerance to these high binders; in contrast, CTLs induced by relatively low HLA-A2-binding epitopes derived from MART-1 or gp100 usually recognize melanoma cells.[21] In this study, all four peptides showed modest binding with HLA-A*2601 and could induce HLA-A26-restricted CTLs from prostate cancer patients.

The HLA-A26 allele is expressed by substantial percentages of populations of varied ethnicity and geography. Among the HLA-A26-positive Japanese population, the frequencies of HLA-A*2601, -A*2602, and A*2603 are 58%, 18%, and 24%, respectively. Therefore, the four peptides identified in this study could be appropriate candidates as cancer vaccines for a relatively large number of patients among Japanese and other ethnic groups. In addition, because they can bind to both HLA-A26 and HLA-A2 (or HLA-A24) molecules, these peptides are expected to be more effective than peptides that only bind to one type of HLA, specifically in patients who carry both HLA-A26 and HLA-A2 (or HLA-A24).

Acknowledgments

Disclosure Statement

The contents are subjected to patent number PCT/JP2008/066589.

References

1 Imanishi T, Akaza T, Kimura A, Tokunaga K, Gojobori T. *Allele and Haplotype Frequencies for HLA and Complement Loci in Various Ethnic Groups*. Oxford, UK: Oxford Scientific Publications, 1992.

2 Niu Y, Komatsu N, Komohara Y et al. A peptide derived from hepatitis C virus (HCV) core protein inducing cellular responses in patients infected with HCV with various HLA class IA alleles. *J Med Virol* 2009; 81: 1232–1240.

3 Mohamed ER, Naito M, Terasaki Y et al. Capability of SART3$_{109-118}$ peptide to induce cytotoxic T lymphocytes from prostate cancer patients with HLA class I-A11, -A31 and -A33 alleles. *Int J Oncol* 2009; 34: 529–36.

4 Matsueda S, Takedatsu H, Yao A et al. Identification of peptide vaccine candidates for prostate cancer patients with HLA-A3 supertype alleles. *Clin Cancer Res* 2005; 11: 6933–43.

5 Pinol-Roma S, Swanson MS, Gall JG, Dreyfuss G. A novel heterogeneous nuclear RNP protein with a unique distribution on nascent transcripts. *J Cell Biol* 1989; 109: 2575–87.

6 Verissimo F, Jordan P. WNK kinases, a novel protein kinase subfamily in multi-cellular organisms. *Oncogene* 2001; 20: 5562–9.

7 Ito M, Shichijo S, Tsuda N et al. Molecular basis of T cell-mediated recognition of pancreatic cancer cells. *Cancer Res* 2001; 61: 2038–46.

8 Mine T, Sato Y, Noguchi M et al. Humoral responses to peptides correlate with overall survival in advanced cancer patients vaccinated with peptides based on pre-existing, peptide-specific cellular responses. *Clin Cancer Res* 2004; 10: 929–37.

9 Takedatsu H, Shichijo S, Azuma K, Sata M, Itoh K. Detection of a set of peptide vaccine candidates for use in HLA-A31+ epithelial cancer patients. *Int J Oncol* 2004; 24: 337–47.

10 Takedatsu H, Shichijo S, Katagiri K, Sawamizu H, Sata M, Itoh K. Identification of peptide vaccine candidates sharing among HLA-A3+, -A11+, -A31+, and -A33+ cancer patients. *Clin Cancer Res* 2004; 10: 1112–20.

11 Rammensee H, Bachmann J, Emmerich NP, Bachor OA, Stevanovic S. SYFPEITHI: database for MHC ligands and peptide motifs. *Immunogenetics* 1999; 50: 213–9.

12 Neumann-Haefelin C, Killinger T, Timm J et al. Absence of viral escape within a frequently recognized HLA-A26-restricted CD8+ T-cell epitope targeting the functionally constrained hepatitis C virus NS5A/5B cleavage site. *J Gen Virol* 2007; 88: 1986–91.

13 Yang D, Nakao M, Shichijo S et al. Identification of a gene coding for a protein possessing shared tumor epitopes capable of inducing HLA-A24-restricted cytotoxic T lymphocytes in cancer patients. *Cancer Res* 1999; 59: 4056–63.

14 Murayama K, Kobayashi T, Imaizumi T et al. Expression of the SART3 tumor-rejection antigen in brain tumors and induction of cytotoxic T lymphocytes by its peptides. *J Immunother* 2000; 23: 511–8.

15 del Guercio MF, Sidney J, Hermanson G et al. Binding of a peptide antigen to multiple HLA alleles allows definition of an A2-like supertype. *J Immunol* 1995; 154: 685–93.

16 Sidney J, Grey HM, Southwood S et al. Definition of an HLA-A3-like supermotif demonstrates the overlapping peptide-binding repertoires of common HLA molecules. *Hum Immunol* 1996; 45: 79–93.

17 Torikai H, Akatsuka Y, Miyauchi H et al. The HLA-A*0201-restricted minor histocompatibility antigen HA-1H peptide can also be presented by another HLA-A2 subtype, A*0206. *Bone Marrow Transplant* 2007; 40: 165–74.

18 Terasaki Y, Shichijo S, Niu Y et al. An HLA-A3-binding prostate acid phosphatase-derived peptide can induce CTLs restricted to HLA-A2 and -A24 alleles. *Cancer Immunol Immunother* 2009; DOI 10.1007/s00262-009-0699-2.

19 Takiguchi M, Matsuda T, Tomiyama H, Miwa K. Analysis of three HLA-A*3303 binding peptide anchors using an HLA-A*3303 stabilization assay. *Tissue Antigens* 2000; 55: 296–302.

20 Nakao M, Yamana H, Imai Y et al. HLA A2601-restricted CTLs recognize a peptide antigen expressed on squamous cell carcinoma. *Cancer Res* 1995; 55: 4248–52.

21 Kawakami Y, Rosenberg SA. T-cell recognition of self peptides as tumor rejection antigens. *Immunol Res* 1996; 15: 179–90.
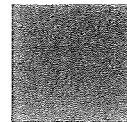
The bcl2 −938CC Genotype Has Poor Prognosis and Lower Survival in Renal Cancer

Hiroshi Hirata, Yuji Hinoda, Koichi Nakajima, Nobuyuki Kikuno, Yutaka Suehiro, Z. Laura Tabatabai, Nobuhisa Ishii and Rajvir Dahiya*

From the Departments of Urology (HH, NK, RD) and Pathology (ZLT), San Francisco Veterans Affairs Medical Center and University of California-San Francisco, San Francisco, California, and Department of Oncology and Laboratory Medicine, Yamaguchi University Graduate School of Medicine (YH, YS), Yamaguchi and Department of Urology, Toho University Faculty of Medicine (KN, NI), Tokyo, Japan

Purpose: A single nucleotide polymorphism (−938C/A, rs2279115) was found in the *bcl2* gene, whose −938A allele is significantly associated with increased Bcl2 expression compared with that of the C allele. Bcl2 up-regulation was reported to be associated with longer survival in patients with renal cancer. However, to our knowledge there is currently no information on the role of the *bcl2*-938C/A single nucleotide polymorphism in renal cell carcinoma cases. Therefore, we investigated the polymorphism at the *bcl2* −938C/A site and its effects on clinical characteristics in patients with renal cell carcinoma.

Materials and Methods: We genotyped the *bcl2*-938C/A single nucleotide polymorphism in 216 patients with renal cancer, and in 209 healthy age and gender matched controls. We also investigated the relationship between the *bcl2* −938C/A polymorphism, Bcl2 expression, proliferation and apoptosis status in renal cell carcinoma tissues using immunohistochemistry and TUNEL assay. The association of the *bcl2* −938C/A single nucleotide polymorphism with survival in patients with renal cell carcinoma was also analyzed by Kaplan-Meier curves.

Results: Survival in Bcl2 positive cases was significantly longer than in negative cases. On univariate and multivariate analyses the *bcl2* −938CC genotype was independently associated with poor prognosis. Kaplan-Meier analysis showed that survival in patients with CC genotypes was significantly worse than in those with CA+AA genotypes. CC genotype carriers had significantly lower Bcl2 expression and higher proliferative activity in renal cancer tissues than CA+AA genotype carriers.

Conclusions: To our knowledge this is the first report to show that the *bcl2* −938C/C genotype has worse prognosis and lower survival in patients with renal cell carcinoma. In addition, the *bcl2* −938C/A single nucleotide polymorphism was shown to be an independent adverse prognostic factor for renal cell carcinoma.

Abbreviations and Acronyms

Bcl2 = B-cell lymphoma

IHC = immunohistochemistry

PCR = polymerase chain reaction

PI = proliferation index

RCC = renal cell carcinoma

RFLP = restriction fragment length polymorphism

SNP = single nucleotide polymorphism

Key Words: kidney; carcinoma, renal cell; polymorphism, single nucleotide; apoptosis; genotype

AMONG urological tumors RCC is the third leading cause of death, accounting for about 2% of adult malignancies.[1] Although the detection rate of RCC has increased with improved diagnostic techniques, metastatic lesions are still found at diagnosis in about 25% of patients with RCC. Moreover, in patients with RCC distant metastasis is sometimes found

721

long after surgical removal of the primary tumor. After detecting these metastases the 5-year survival rate is generally less than 10%.[2] Standard treatment for localized renal cancer is surgical removal, while immunotherapy is used for metastatic disease because of its multidrug resistance. Interleukin-2 was the most common immunotherapy for RCC but it was effective in only 10% to 15% of patients.[2,3] Recently targeted tyrosine kinase inhibitors have been used for advanced RCC with improved progression-free and overall survival compared with that of interferon treatment.[4]

Bcl2 family proteins, which are well-known as mitochondrial membrane proteins, are important regulators of programmed cell death or apoptosis in normal tissues and cancer cells.[5] Bcl2 family proteins contain anti-apoptotic proteins such as Bcl2 and Bcl-xL, and pro-apoptotic proteins such as Bax and Bak.[5] High Bcl2 expression is associated with poor survival in several different cancers, including B-cell chronic lymphocytic leukemia, prostate cancer and urinary tract transitional cell cancer.[6–8] In contrast, Bcl2 up-regulation is associated with longer survival in various cancers, including colon, breast and nonsmall cell lung cancer.[9–12] In RCC cases previous studies have shown an association between increased Bcl2 expression and better prognosis.[13,14]

The bcl2 gene, which is located on chromosome 18q21.3, consists of 3 exons and the 2 promoters P1 and P2.[13] Interestingly these promoters have different functions. P2, located 1400 bp upstream of the translation initiation site, decreases the activity of P1 promoter function.[15]

A novel functional single nucleotide polymorphism (−938C/A, rs2279115) was found in the P2 negative regulatory element. The −938C allele was significantly associated with increased P2 promoter activity and binding of nuclear proteins compared with the A allele, resulting in overall decreased bcl2 promoter transcriptional activity.[16] Bcl2 protein expression in patients with chronic lymphocytic leukemia who carry the −938C/C genotype is significantly decreased compared to that in patients with the −938A/A genotype.[16]

Therefore, due to this evidence we hypothesized that 1) the bcl2 promoter −938C/A polymorphism may increase Bcl2 expression in renal cancer tissues, 2) increased Bcl2 expression may be associated with longer survival in patients with RCC and 3) the bcl2 −938C/A polymorphism may be an important prognostic indicator in patients with RCC. To test these hypotheses we performed a case-control study genotyping the polymorphic site in bcl2 −938C/A. We also investigated the relationship between Bcl2 expression in RCC tissues and genotypes with the bcl2 −938C/A polymorphism. In addition, we exam-

ined the relationship between the bcl2 −938C/A polymorphism and apoptosis/proliferation status in RCC tissues using the TUNEL assay and Ki-67 IHC.

MATERIALS AND METHODS

Samples
Genomic DNA was extracted from peripheral blood in 160 patients and from paraffin embedded noncancerous kidney tissue in 56 as well as from 209 healthy individuals. A DNA mini kit (QIAgen®) was used to extract DNA from normal tissue and peripheral blood according to manufacturer protocols. A total of 149 male and 67 female patients with pathologically confirmed conventional RCC, and 209 age and sex matched controls were enrolled in this study. Mean age in patients and controls was 62.2 and 61.6 years, respectively (ANOVA $p = 0.62$, table 1). All 216 patients tested were diagnosed with RCC based on histopathological findings. Disease was classified according to WHO criteria and staged according to the TNM classification. Healthy controls consisted of volunteers with no apparent abnormal findings upon medical examination at Shimane University Hospital. Peripheral blood samples were obtained from patients and controls after written informed consent was obtained at Shimane University Hospital and Toho University Hospital. This study was approved by Shimane Medical University and Toho University. Study samples were previously reported.[17]

Genotyping
Polymorphisms were analyzed by PCR-RFLP. The PCR primers used for bcl2 were GCGTCCTGCCTTCATTTATC

Table 1. Characteristics of patients with RCC and controls

	No. Pts	No. Controls (%)
Overall	216	209
Mean ± SD age*	62.2 ± 12	61.6 ± 14
Gender:†		
M	149 (69)	149 (71)
F	67 (31)	60 (29)
Grade:		
1	52 (24.1)	
2	137 (63.4)	
3 + 4	27 (12.5)	
pT:		
1	117 (54.2)	
2	46 (21.3)	
3	50 (23.1)	
4	3 (1.4)	
pN:		
Neg	199 (92.1)	
Pos	17 (7.9)	
pM:		
Neg	192 (88.9)	
Pos	24 (11.1)	
Pathological findings:		
Clear cell Ca	203 (94.0)	
Granular cell Ca	11 (5.1)	
Chromophobe cell Ca	2 (0.9)	

* p = 0.62.
† p = 0.55.

138